Quasi-Cyclic Symbol Extensions for Shaping the OFDM Spectrum

Tayebeh Taheri, Rickard Nilsson, and Jaap van de Beek, *Fellow, IEEE*

***Abstract*— N-continuous orthogonal frequency division multiplexing (OFDM) is a promising solution to the out-of-band (OOB) emission issue in OFDM systems where the Nth-order continuity between OFDM symbols leads to lower OOB emission than the plain OFDM; however, high self-interference in such systems is an obstacle. In this paper, we propose a new class of quasi-cyclic symbol extensions, which makes the OFDM system N-continuous. The new extension leads to low OOB emission while the additive interference is less than other N-continuous OFDM systems. Moreover, we propose a general analysis of the spectrum and interference that occurs in a linear precoded OFDM system. The framework is applicable to many N-continuous OFDM systems including our proposed method.**

***Index Terms*— OFDM, spectral precoding, out-of-band emission, interference, PAPR.**

I. Introduction

With the heavily growing number of wireless devices, the sub-6 GHz spectrum is becoming increasingly congested. Most of the radio spectrum is already occupied or licensed; therefore, there is an increasing need for efficient use of the spectrum. Cognitive radio is a solution for the spectrum crowding problem allowing unlicensed users use the temporary unused gaps of the spectrum. Orthogonal frequency-division multiplexing (OFDM) is the waveform which has been used in fourth generation (4G) systems. On the process to choose a waveform for fifth generation (5G) communication systems, completely new waveforms were proposed, for example, Filter Bank Multicarrier (FBMC) [1], Universal Filtered MultiCarrier (UFMC) [2] and Generalised Frequency Division Multiplexing (GFDM) [3]. A comprehensive overview of candidate waveforms for 5G networks is presented in [4]. However, recentely, 3GPP decided to continue with OFDM in 5G communication technologies [5]. OFDM provides a suitable scheme for cognitive radio scenarios because it embodies a straightforward flexible way to shape the spectrum by deactivating unused subcarriers. However, OFDM systems suffer from high out-of-band (OOB) emission potentially leading to severe radiation to adjacent bands. Therefore, in coming communications systems and cognitive radio scenarios where many different radio-systems co-exist, residual OOB emissions need special attention. Several methods have been proposed in the literature to suppress the OOB emission including filtering [6], time domain transmit-windowing [7]–[11] and, more recently, N-continuous OFDM [12]–[17].

Since the OFDM symbol is a multiplex of rectangularly windowed sinusoids, its signal trajectory is discontinuous. The sharp edges of adjacent OFDM symbols are a reason for high OOB emissions. A classical means to suppress the OOB emission is smoothing the signal by low-pass filtering of the baseband OFDM signal [6]. Time domain transmit-windowing is another classical approach that suppresses the OOB emission by shaping the sharp boundaries of the two consecutive OFDM symbols by applying a smooth window to the OFDM symbol. This method is used for long in digital subscriber line (DSL) systems [19]. This technique is also allowed in vendor-proprietary implementations of the current LTE standard [20].

Another method to suppress the OOB emission which shapes OFDM symbols is N-continuous OFDM. N-continuity is a signal property in which symbols are forced continuous up to N^{th}-order derivatives. There are many ways to construct N-continuity, see for example [12]–[17].

The N^{th}-order continuity between OFDM symbols leads to lower OOB emission compared to plain, uncoded OFDM, shown in Figure 1a [18]. The very first idea of N-continuous OFDM was introduced in [12] and extended in [13] where a precoder manipulates the OFDM data symbol in order to make the signal N-continuous, see Figures 1b and 1c. N-continuous OFDM in [12] and [13] modify the whole OFDM symbol by slightly changing the whole data symbol through a pre-FFT symbol precoder. In [12] a precoder with memory was developed where the precoder forces the current symbol to be connected to the previous symbol, up to N^{th}-order derivatives, knowing the previous data symbol. In [13] an associated memoryless precoder was presented. The scheme in [13] solves the memory issue by forcing the end and beginning of each symbol to zero, up to N^{th}-order derivatives; therefore, the consecutive symbols become N-continuous. The N-continuous precoders in [12] and [13] have the same performance [13]. We will denote the precoding systems which change the whole data symbol, including the method in [13] and Figure 1c, as *symbol precoding*. Symbol precoding causes the OFDM subcarriers to lose their orthogonality, and therefore self-interference appears in the receiver. Moreover, as in plain OFDM, a long multipath channel, longer than cyclic prefix, causes leakage from a previous symbol into the current symbol

Manuscript received December 7, 2017; revised May 22, 2018; accepted July 30, 2018. Date of publication August 22, 2018; date of current version October 9, 2018. This work was supported by the Swedish Research Council under Grant 2014-5977. The associate editor coordinating the review of this paper and approving it for publication was L. Song. *(Corresponding author: Tayebeh Taheri.)*

The authors are with the Department of Computer Science, Electrical and Space Engineering, LuleåUniversity of Technology, SE97187 Luleå, Sweden (e-mail: tayebeh.taheri@ltu.se; rickard.o.nilsson@ltu.se; jaap.vandebeek@ltu.se).

Color versions of one or more of the figures in this paper are available online at http://ieeexplore.ieee.org.

Digital Object Identifier 10.1109/TWC.2018.2865566

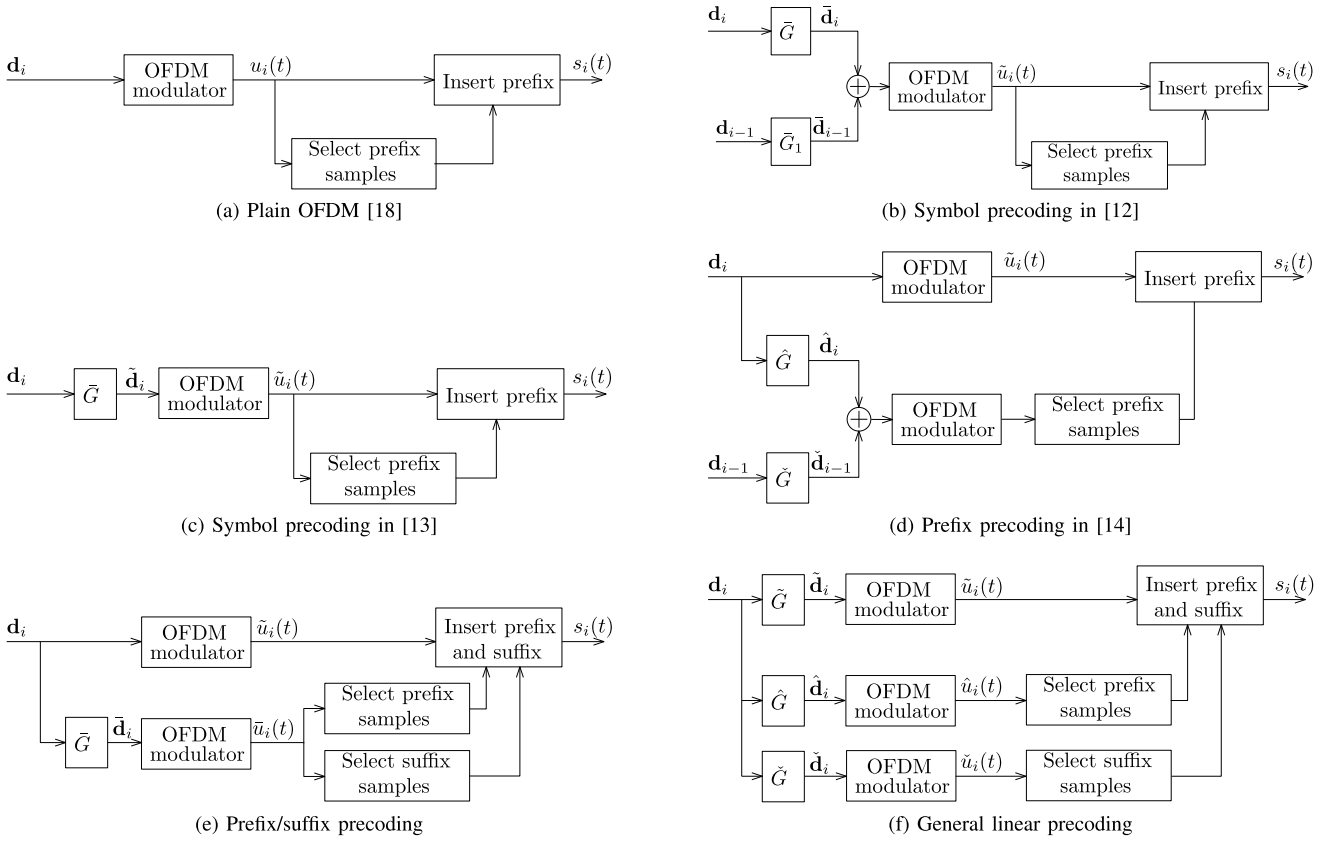

(a) Plain OFDM [18]

(b) Symbol precoding in [12]

(c) Symbol precoding in [13]

(d) Prefix precoding in [14]

(e) Prefix/suffix precoding

(f) General linear precoding

Fig. 1. The transmitters' block diagrams of a) plain, b) symbol precoding in [12], c) symbol precoding in [13], d) prefix precoding in [14] e) prefix/suffix precoding and f) general linear precoding OFDM systems. The precoder $\tilde{\mathbf{G}}$, $\hat{\mathbf{G}}$ and $\check{\mathbf{G}}$ are different for each system.

known as intersymbol interference (ISI). In case of a short dispersive channel, the presence of a cyclic prefix preserves the orthogonality between subcarriers by making the effective part of the symbol be a circular convolution of transmitted signal by the channel impulse response. A long dispersive channel also causes loss of orthogonality between subcarriers known as intercarrier interference (ICI).

In contrast, recently a new idea has emerged in [14] which inserts N-continuous OFDM correction symbols *only* into the guard interval, see Figure 1d. Therefore, no self-interference occurs, at the price of an increased sensitivity to channel-induced ISI and ICI. However, a proper analysis of the price paid in terms of ISI and ICI is missing in [14]. Moreover, precoder in [14] needs the information of the previous symbol to construct the continuity which means extra memory consumption. We refer to the precoding approach which changes the symbol just in prefix part, including the precoding method in [14] and Figure 1d, as *prefix precoding*.

This paper has three contributions: first, inspired by the ideas in [14], we propose a precoder which results in a new class of symbol extensions that makes the signal N-continuous in a memoryless fashion. In a sense our paper now repeats the development made from [12] to [13]. Because we explicitly introduce both a prefix and a suffix, and the new precoder changes the data symbol only in the extension parts, we refer to this approach as *prefix/suffix precoding*, see Figure 1e. Although the proposed precoder changes prefix and suffix, the changes are small and therefore, prefix and suffix are *almost* cyclic. We will see that our system provides good OOB emission suppression with less amount of interference than symbol precoding in [12] and [13] and prefix precoding in [14].

Secondly, we develop a general analysis framework both at the transmitter and receiver side Figure 1f shows a general linear precoding model that we analyse in this paper. We show that the systems in Figures 1a,c-d are special cases of Figure 1f. Using the developed framework we give expressions for both interference and power spectrum in a general linearly precoded system. In the literatures [12]–[14] there is lack of the interference analysis of the precoded systems. We evaluate the interference for precoders in [13] and [14] and compare the results with interference in the new prefix/suffix precoded system. We also show that the rate-loss due to precoding in the prefix/suffix precoded system is very small compared with rate-loss in the plain OFDM system.

Thirdly, we discuss the similarities and differences between N-continuous OFDM and transmit-windowing. While [9] presents analysis of interference that occurs in a transmit-windowed OFDM system, we here look at the symbol shaping strategy of each method. Moreover, we look at the Peak-to-Average Power Ratio (PAPR) of an N-continuous OFDM. We also show that for both prefix precoding and prefix/suffix precoding methods the complexity increases linearly with the number of subcarriers.

In Section II we present a system model for a general linear precoded OFDM system. Section III introduces special cases

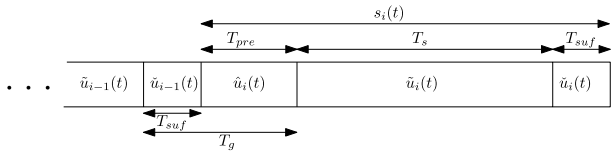

(a) Prefix and suffix share the guard interval, $T_{\text{pre}}=(1-\beta)T_g$ and $T_{\text{suf}}=\beta T_g$ where $0<\beta<1$.

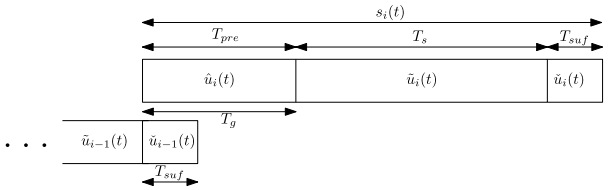

(b) Prefix and suffix overlap over the guard interval, $T_{\text{pre}}=T_g$ and $T_{\text{suf}}\leq T_g$.

Fig. 2. Transmit precoded OFDM signal.

of the general precoded OFDM systems In Subsection III-B, we introduce a new memoryless prefix/suffix precoder which makes the system N-continuous and suppresses the OOB emission with less amount of overall interference than precoding in [13] and [14]. We analyse the transmitted power spectrum of the general precoded OFDM system in Section IV and in Section V we analyse the interference that occurs in such systems in case of a dispersive channel. In Section VI, we evaluate the spectrum properties of the proposed prefix/suffix precoder and the interference in our system. We also compare our results of prefix/suffix precoding with results of symbol precoding in [13] and prefix precoding in [14]. We evaluate the achievable rate in a prefix/suffix precoded OFDM system in Section VII and finally, time domain transmit-windowing and its similarities and differences with an N-continuous OFDM, PAPR in N-continuous OFDM systems and complexity of the proposed method are discussed in Section VIII.

II. System Model

We first write the transmitted signal as

$$s(t) = \sum_i s_i(t - i(T_s + T_g)), \tag{1}$$

where $s_i(t)$ is the ith OFDM symbol, T_s is the useful part of the OFDM symbol and T_g is a fixed-length guard interval between consecutive symbols. The OFDM symbol in (1) is extended by a fixed-length prefix with a duration of T_{pre} and a fixed-length suffix with a duration of T_{suf}. Symbol extension by the suffix was introduced for the first time in [21]. We consider two scenarios of extending the OFDM symbols in the guard intervals. The first scenario is that the prefix of current symbol and suffix of the previous symbol share the guard interval without overlapping, $T_g = T_{\text{pre}}+T_{\text{suf}}$, see Figure 2a. In the second scenario the prefix of the current symbol and the suffix of the previous symbol overlap in the guard interval, see Figure 2b, usually in such a case $T_{\text{pre}} = T_g$. In what follows we will explicitly refer whatever scenario is being discussed.

We write $s_i(t)$ as a sum of three signal components, these components represent the signal in the useful, prefix and suffix parts,

$$s_i(t)=\tilde{u}_i(t)I_{[0,T_s)}(t)+\hat{u}_i(t)I_{[-T_{\text{pre}},0)}(t) + \check{u}_i(t)I_{[T_s,T_s+T_{\text{suf}})}(t) \tag{2}$$

where $I_X(t)$ is the indicator function: $I_X(t) = 1$ for $t \in X$ and zero otherwise, and

$$\tilde{u}_i(t) = \sum_{k\in\mathcal{K}} \tilde{d}_{i,k} e^{j2\pi \frac{k}{T_s} t}, \quad \hat{u}_i(t) = \sum_{k\in\mathcal{K}} \hat{d}_{i,k} e^{j2\pi \frac{k}{T_s} t},$$

and

$$\check{u}_i(t) = \sum_{k\in\mathcal{K}} \check{d}_{i,k} e^{j2\pi \frac{k}{T_s} t}. \tag{3}$$

Data symbols $\tilde{d}_{i,k}$, $\hat{d}_{i,k}$ and $\check{d}_{i,k}$ are the results of a precoding step. The purpose of the precoding is to reduce the OOB emission. Therefore, in vector notation,

$$\tilde{\mathbf{d}}_i = \tilde{\mathbf{G}}\mathbf{d}_i, \quad \hat{\mathbf{d}}_i = \hat{\mathbf{G}}\mathbf{d}_i \text{ and } \check{\mathbf{d}}_i = \check{\mathbf{G}}\mathbf{d}_i. \tag{4}$$

Here $\mathcal{K}=\{k_1, k_2, \ldots, k_K\}$ is the set of subcarrier indices, $\mathbf{d}_i = [d_{i,1}, d_{i,2}, \ldots, d_{i,K}]^T$ represents information data taken from a symbol constellation. The vectors $\tilde{\mathbf{d}}_i = [\tilde{d}_{i,1}, \tilde{d}_{i,2}, \ldots, \tilde{d}_{i,K}]^T$, $\hat{\mathbf{d}}_i = [\hat{d}_{i,1}, \hat{d}_{i,2}, \ldots, \hat{d}_{i,K}]^T$ and $\check{\mathbf{d}}_i = [\check{d}_{i,1}, \check{d}_{i,2}, \ldots, \check{d}_{i,K}]^T$ contain the precoded data symbols using size-$K\times K$ matrices $\tilde{\mathbf{G}}$, $\hat{\mathbf{G}}$ and $\check{\mathbf{G}}$ which represent precoders for the useful part of the symbol, the prefix and the suffix part of the symbol, respectively. This model generalizes earlier models in the literature, [12]–[14], by explicitly separating the precoding of the useful signal part (through $\tilde{\mathbf{G}}$) and its prefix and suffix (through $\hat{\mathbf{G}}$ and $\check{\mathbf{G}}$). Various known models appear as special cases.

III. Three Special Cases and One New Precoder

A. Special Cases

In general $\tilde{\mathbf{G}}$, $\hat{\mathbf{G}}$ and $\check{\mathbf{G}}$ are not equal and unique for each system. In this Section we will show that systems in Figures 1a, c-d have a system model of in Section II; therefore all are special cases of the system in Figure 1f.

1) Plain OFDM: In case of plain OFDM in Figure 1a [18], usually symbols are extended only by a fixed-length prefix, $T_g = T_{\text{pre}}$ and $T_{\text{suf}} = 0$. In plain OFDM, all precoders are identity matrices, $\tilde{\mathbf{G}} = \hat{\mathbf{G}} = \check{\mathbf{G}} = \mathbf{I}$. Note that in plain OFDM the prefix is a cyclic extension of the useful symbol.

2) Symbol Precoding [13]: The symbol is extended using a fixed-length prefix, $T_g = T_{\text{pre}}$ and $T_{\text{suf}} = 0$. Moreover, the useful part of the symbol and prefix are precoded by the same precoder and the prefix remains cyclic, the precoded prefix is cyclic to the precoded OFDM symbol. As $T_{\text{suf}} = 0$, there is no need to define any $\check{\mathbf{G}}$. Symbol precoding

in Figure 1c [13], uses a precoder $\bar{\mathbf{G}}$ to force the beginning and end of each symbol to zero up to N_c[th]-order derivatives,

$$\bar{\mathbf{d}}_i = \bar{\mathbf{G}}\mathbf{d}_i, \quad \bar{\mathbf{G}} = \mathbf{I} - \bar{\mathbf{A}}^H(\bar{\mathbf{A}}\bar{\mathbf{A}}^H)^{-1}\bar{\mathbf{A}},$$
$$where \quad \bar{\mathbf{A}} = \begin{bmatrix} \mathbf{A}\mathbf{\Phi}_{\text{pre}} \\ \mathbf{A} \end{bmatrix}. \tag{5}$$

Here $\mathbf{\Phi}_{\text{pre}} = \text{diag}(e^{j\phi_{\text{pre}}k_1}, \ldots, e^{j\phi_{\text{pre}}k_K})$, $\phi_{\text{pre}} = -2\pi T_{\text{pre}}/T_s$ and $\mathbf{A}$ is a $(N_c+1)\times K$ matrix,

$$\mathbf{A} = \begin{bmatrix} 1 & 1 & \ldots & 1 \\ k_1 & k_2 & \ldots & k_K \\ \vdots & \vdots & & \vdots \\ k_1^{N_c} & k_2^{N_c} & \ldots & k_K^{N_c} \end{bmatrix}. \tag{6}$$

The precoder $\bar{\mathbf{G}}$ changes the whole data symbol including the prefix and useful part of the symbol, see Figure 1c.

Symbol precoding is a special case of Figure 1f with the transmitted signal as (1) with $\tilde{\mathbf{G}} = \hat{\mathbf{G}} = \bar{\mathbf{G}}$.

3) Prefix Precoding: In prefix precoding in [14] the useful part of the symbol is unchanged while the current data, $\mathbf{d}_i$, and previous data, $\mathbf{d}_{i-1}$, are combined to construct the data symbol in prefix part as

$$\mathbf{d}_i^{\text{pre}} = (\mathbf{I} - \mathbf{P})\mathbf{d}_i + \mathbf{P}\mathbf{\Phi}^H\mathbf{d}_{i-1}, \tag{7}$$

where $\mathbf{d}_i^{\text{pre}} = [d_{i,1}^{\text{pre}}, d_{i,2}^{\text{pre}}, \ldots, d_{i,K}^{\text{pre}}]^T$ is the data in prefix part and

$$\mathbf{P} = \begin{bmatrix} \mathbf{A}\mathbf{\Phi}_{\text{pre}} \\ \mathbf{A} \end{bmatrix}^{\dagger} \begin{bmatrix} \mathbf{A}\mathbf{\Phi}_{\text{pre}} \\ \mathbf{0}_{(N+1)\times K} \end{bmatrix} \tag{8}$$

and $\mathbf{\Phi}_{\text{pre}} = \text{diag}(e^{j\phi_{\text{pre}}k_1}, \ldots, e^{j\phi_{\text{pre}}k_K})$, $\phi_{\text{pre}} = -2\pi T_{\text{pre}}/T_s$. Here, $[.]^{\dagger}$ represents the Moore-Penrose pseudo inverse and $\mathbf{A}$ is a $(N_c+1)\times K$ matrix in (6). In prefix precoding the whole guard interval is used as a prefix, $T_g = T_{\text{pre}}$. Changing the prefix using (7) makes the consecutive OFDM symbols continuous up to N_c[th]-order derivatives.

Lemma 1: The prefix precoder in Figure 1d [14] is identical to a linear prefix/suffix precoder with the transmitted signal as (1) with

$$\tilde{\mathbf{G}} = \mathbf{I}, \quad \hat{\mathbf{G}} = \mathbf{I} - \mathbf{P}, \text{ and } \check{\mathbf{G}} = \mathbf{P}\mathbf{\Phi}_{pre}^H, \tag{9}$$

where prefix of a current symbol and suffix of previous symbol have the same length and overlap over the whole guard interval, $T_g = T_{pre} = T_{suf}$.

The proof is given in the appendix. The prefix precoder in Figure 1d uses two precoders to construct the data for the prefix part, $\mathbf{d}_i^{\text{pre}} = \hat{\mathbf{G}}\mathbf{d}_i + \check{\mathbf{G}}\mathbf{d}_{i-1}$, where $\mathbf{d}_i^{\text{pre}}$ is the data in prefix part. One of the precoders, $\hat{\mathbf{G}}$, is applied to the current data symbol and the other one, $\check{\mathbf{G}}$, is applied to the previous data symbol. In order to make the prefix precoding system compatible with our model in Section II, instead of precoding a prefix as a combination of current and previous data symbols, we extend each symbol by a prefix and a suffix and precode each part independently, see Figure 1f. Here, the prefix of the current symbol and the suffix of the previous symbol have the same length and overlap over the whole guard interval, $T_g = T_{\text{pre}} = T_{\text{suf}}$. Simulations in Section VI show the identical results. Note that in prefix precoding the useful part of the symbol is not precoded, therefore, $\tilde{\mathbf{G}} = \mathbf{I}$.

B. A New Precoder: Prefix/Suffix Precoding

In this section we propose a new precoder which makes the signal N-continuous by changing the data symbol only in prefix and suffix part. Here, because we want to keep the useful part of the symbol unchanged, $\tilde{\mathbf{d}}_i$=$\mathbf{d}_i$, we choose $\tilde{\mathbf{G}}$=$\mathbf{I}$. We consider that the prefix and the suffix are precoded using the same precoder $\bar{\mathbf{G}}$, $\hat{\mathbf{G}} = \check{\mathbf{G}} = \bar{\mathbf{G}}$, and $\bar{\mathbf{d}}_i = \bar{\mathbf{G}}\mathbf{d}_i$ where $\bar{\mathbf{d}}_i = [\bar{d}_{i,1}, \bar{d}_{i,2}, \ldots, \bar{d}_{i,K}]^T$ contain the precoded data symbols, see Figure 1e. This is the first difference between the new precoder and the prefix precoder in [14] which uses two different precoders for the prefix, $\hat{\mathbf{G}}$, and the suffix part, $\check{\mathbf{G}}$. Even though the new precoder is the same for the prefix and suffix part, but the prefix and the suffix will be different because the indicator functions in (2), $I_{[-T_{\text{pre}},0)}(t)$ and $I_{[T_s,T_s+T_{\text{suf}})}(t)$, are not the same. Note that here, $\bar{\mathbf{G}}$ is different from the precoder in (5). Precoder $\bar{\mathbf{G}}$ is calculated under the following constraints

$$\frac{d^n}{dt^n}\hat{u}_i(t)\Big|_{t=-T_{\text{pre}}} = 0 \tag{10}$$

$$\frac{d^n}{dt^n}\hat{u}_i(t)\Big|_{t=0} = \frac{d^n}{dt^n}\tilde{u}_i(t)\Big|_{t=0} \tag{11}$$

$$\frac{d^n}{dt^n}\check{u}_i(t)\Big|_{t=T_s} = \frac{d^n}{dt^n}\tilde{u}_i(t)\Big|_{t=T_s} \tag{12}$$

$$\frac{d^n}{dt^n}\check{u}_i(t)\Big|_{t=T_s+T_{\text{suf}}} = 0 \tag{13}$$

for each $n \in \{0, 1, \ldots, N_c\}$, N_c is the order of the continuity. These constraints make the signal continuous by forcing the signal at edges of the prefix and the suffix to be continuous. The idea is to design a memoryless precoder. Constraints (10) and (13) form the new precoder as a memoryless precoder as opposed to prefix precoder in [14] which needs the information of the previous symbol to construct the continuity. After some computation similar to [12], (11) and (12) reduce to a same constraint. The three remaining constraints can be expressed in matrix form as

$$\bar{\mathbf{A}}\bar{\mathbf{d}}_i = \bar{\mathbf{B}}\mathbf{d}_i, \tag{14}$$

where

$$\bar{\mathbf{A}} = \begin{bmatrix} \mathbf{A}\mathbf{\Phi}_{\text{pre}} \\ \mathbf{A} \\ \mathbf{A}\mathbf{\Phi}_{\text{suf}} \end{bmatrix} \quad \text{and} \quad \bar{\mathbf{B}} = \begin{bmatrix} \mathbf{0}_{(N_c+1)\times K} \\ \mathbf{A} \\ \mathbf{0}_{(N_c+1)\times K} \end{bmatrix}. \tag{15}$$

Here $\mathbf{\Phi}_{\text{pre}} = \text{diag}(e^{j\phi_{\text{pre}}k_1}, \ldots, e^{j\phi_{\text{pre}}k_K})$, $\phi_{\text{pre}} = -2\pi T_{\text{pre}}/T_s$ and $\mathbf{\Phi}_{\text{suf}} = \text{diag}(e^{j\phi_{\text{suf}}k_1}, \ldots, e^{j\phi_{\text{suf}}k_K})$, $\phi_{\text{suf}} = 2\pi T_{\text{suf}}/T_s$ and $\mathbf{A}$ is a $(N_c+1)\times K$ matrix in (6).

We are interested only in a solution of equation (14) where $\bar{\mathbf{d}}_i$ is nearest to the information data vector $\mathbf{d}_i$ in a Euclidean sense. The solution to (14) is

$$\bar{\mathbf{d}}_i = \bar{\mathbf{G}}\mathbf{d}_i, \quad \bar{\mathbf{G}} = \mathbf{I} - \bar{\mathbf{A}}^H(\bar{\mathbf{A}}\bar{\mathbf{A}}^H)^{-1}(\bar{\mathbf{A}} - \bar{\mathbf{B}}). \tag{16}$$

where $\bar{\mathbf{G}}$ is the new $K\times K$ prefix/suffix precoding matrix.

The precoder $\bar{\mathbf{G}}$ changes the symbol only in the prefix and suffix part of the symbol and makes the whole signal continuous with unchanged data symbol in the useful part, $\tilde{\mathbf{d}}_i$=$\mathbf{d}_i$.

IV. Transmission: Power Spectrum

In this section we derive an analytical expression of the power spectrum of the linear precoded OFDM system (1)–(4). In Section VI we will evaluate the spectrum for symbol precoding in [13], prefix precoding in [14] and our proposed prefix/suffix precoding OFDM systems. We start with writing the Fourier transform of (2) as

$$\begin{aligned} S_i(f) &= \sum_k \tilde{d}_{i,k}\tilde{a}_k(f) + \sum_k \hat{d}_{i,k}\hat{a}_k(f) + \sum_k \check{d}_{i,k}\check{a}_k(f) \\ &= \tilde{\mathbf{a}}^T(f)\tilde{\mathbf{d}}_i + \hat{\mathbf{a}}^T(f)\hat{\mathbf{d}}_i + \check{\mathbf{a}}^T(f)\check{\mathbf{d}}_i = \mathbf{a}^T(f)\mathbf{d}_i, \quad (17) \end{aligned}$$

where, with (4),

$$\mathbf{a}(f) = \tilde{\mathbf{G}}^T\tilde{\mathbf{a}}(f) + \hat{\mathbf{G}}^T\hat{\mathbf{a}}(f) + \check{\mathbf{G}}^T\check{\mathbf{a}}(f), \quad (18)$$

and $\tilde{\mathbf{a}}(f) = (\tilde{a}_{k_1}(f), \tilde{a}_{k_2}(f), \ldots, \tilde{a}_{k_K}(f))^T$, $\hat{\mathbf{a}}(f) = (\hat{a}_{k_1}(f), \hat{a}_{k_2}(f), \ldots, \hat{a}_{k_K}(f))^T$ and $\check{\mathbf{a}}(f) = (\check{a}_{k_1}(f), \check{a}_{k_2}(f), \ldots, \check{a}_{k_K}(f))^T$, $\tilde{a}_k(f)$, $\hat{a}_k(f)$ and $\check{a}_k(f)$ are the Fourier transforms of $e^{j2\pi\frac{k}{T_s}t}I_{[0,T_s)}$, $e^{j2\pi\frac{k}{T_s}t}I_{[-T_{\text{pre}},0)}$ and $e^{j2\pi\frac{k}{T_s}t}I_{[T_s,T_s+T_{\text{suf}})}$ respectively.

The power spectrum $P(f)$ of (1) is then [22]

$$P(f) = \frac{1}{T}E\{|S_i(f)|\}^2 = \frac{1}{T}\|\mathbf{a}(f)\|_2^2, \quad (19)$$

where the expectation $E\{\cdot\}$ is over all possible transmitted OFDM symbols. In the second quality, we assume that the data are uncorrelated, $E\{\mathbf{d}_i\mathbf{d}_i^H\}=\mathbf{I}_K$ and $E\{\mathbf{d}_i\mathbf{d}_j^H\}=\mathbf{0}_K$ if $i\neq j$.

As we expect the power spectrum (19) depends on all precoders $\tilde{\mathbf{G}}$, $\hat{\mathbf{G}}$ and $\check{\mathbf{G}}$. Later in Section VI we evaluate (19) for prefix/suffix precoded system and we will see that (19) has low OOB emission similar to symbol precoding OFDM in [13] and prefix precoding OFDM in [14].

V. Reception: Interference Analysis

For the sake of the receiver interference analysis, we now adopt a discrete-time model at the receiver where $s[n]$ is the discrete-time transmitted signal. We transmit $s[n]$ over a dispersive channel with impulse response $h[n]$ of length H, $\mathbf{h}=[h_1 \ldots h_H, 0, 0, \ldots, 0]$. We are interested in the interference in precoded OFDM systems that occurs when the length of $h[n]$ exceeds the length of the prefix, which is likely to be the dominant scenario in for instance low-latency 5G systems where short symbol-extensions are likely to be used for the sake of low latency. Our analysis is based on the interference resulting from one particular channel impulse response. Later, in our simulations, we evaluate the *average* interference in the OFDM signal (1).

The discrete-time equivalent of the ith transmitted symbol (2) can be presented in matrix form,

$$\mathbf{s}_i = \mathbf{T}_1\tilde{\mathbf{u}}_i + \mathbf{T}_2\hat{\mathbf{u}}_i + \mathbf{T}_3\check{\mathbf{u}}_i, \quad (20)$$

where $\tilde{\mathbf{u}}_i=\mathbf{F}^H\tilde{\mathbf{d}}_i$ ($\mathbf{F}^H$ is the inverse DFT matrix), $\hat{\mathbf{u}}_i=\mathbf{F}^H\hat{\mathbf{d}}_i$ and $\check{\mathbf{u}}_i=\mathbf{F}^H\check{\mathbf{d}}_i$,

$$\mathbf{T}_1 = \begin{bmatrix} \mathbf{0}_{L_{\text{pre}}\times N} \\ \mathbf{I}_{N\times N} \\ \mathbf{0}_{L_{\text{suf}}\times N} \end{bmatrix}, \quad \mathbf{T}_2 = \begin{bmatrix} \mathbf{0}_{L_{\text{pre}}\times(N-L_{\text{pre}})} & \mathbf{I}_{L_{\text{pre}}} \\ \mathbf{0}_{(N+L_{\text{suf}})\times N} & \end{bmatrix}$$

$$\text{and} \quad \mathbf{T}_3 = \begin{bmatrix} \mathbf{0}_{(N+L_{\text{pre}})\times N} \\ \mathbf{I}_{L_{\text{suf}}} \quad \mathbf{0}_{L_{\text{suf}}\times(N-L_{\text{suf}})} \end{bmatrix}. \quad (21)$$

Equation (20) is the discrete equivalent of (2) where $\tilde{\mathbf{u}}_i$, $\hat{\mathbf{u}}_i$ and $\check{\mathbf{u}}_i$ represents $\tilde{u}_i(t)$, $\hat{u}_i(t)$ and $\check{u}_i(t)$ in matrix form respectively and $\mathbf{T}_1$, $\mathbf{T}_2$ and $\mathbf{T}_3$ are matrix form of rectangular pulses of $I_{[0,T_s)}(t)$, $I_{[-T_{\text{pre}},0)}(t)$ and $I_{[T_s,T_s+T_{\text{suf}})}(t)$ respectively.

We assume that the channel length in shorter than one complete OFDM symbol, therefore, at the receiver, there is only leakage from the previous symbol to the current symbol. Ignoring receiver noise, we write the received symbol vector after the receiver FFT in a general precoded OFDM system as

$$\mathbf{r}_i = \mathbf{F}(\mathbf{H}_1\mathbf{s}_i + \mathbf{H}_2\mathbf{s}_{i-1}) \quad (22)$$

where $\mathbf{r}_i=[r_{i,1} \ldots r_{i,K}]^T$ is a size-$K\times 1$ vector and $\mathbf{F}$ is the $K\times K$ DFT-matrix with entries $[\mathbf{F}]_{xy}=\frac{1}{\sqrt{K}}e^{-2j\pi\frac{xy}{K}}$. Here, $\mathbf{H}_1$ is the size $N\times(N+L_{\text{pre}}+L_{\text{suf}})$ matrix

$$\mathbf{H}_1 = \begin{bmatrix} \begin{bmatrix} h_{L_{\text{pre}}+1} & \cdots & h_2 \\ \vdots & & \vdots \\ h_H & & \\ & \ddots & \\ & & h_H \end{bmatrix} & \begin{bmatrix} h_1 & & \\ \vdots & \ddots & \\ & & \\ & & \\ h_H & & \\ & \ddots & \\ & & h_H \cdots h_1 \end{bmatrix} & \begin{bmatrix} \\ \\ \\ \\ \\ \\ \\ \mathbf{0}_{N\times L_{\text{suf}}} \end{bmatrix} \end{bmatrix}, \quad (23)$$

where N is the number of samples in one OFDM symbol and $L_{\text{pre}}=T_{\text{pre}}N/T_s$ and $L_{\text{suf}}=T_{\text{suf}}N/T_s$ are the number of samples in the prefix and the suffix.

Similar to $\mathbf{H}_1$, $\mathbf{H}_2$ is the size $N\times(N+L_{\text{pre}}+L_{\text{suf}})$ matrix that captures the prefix and suffix residual. If the prefix and suffix share the guard interval, as in Figure 2a, $\mathbf{H}_2$ becomes

$$\mathbf{H}_2 = \begin{bmatrix} 0 & \cdots & 0 & h_H & \cdots & h_{L_{\text{pre}}-L_{\text{suf}}+2} \\ \vdots & & & & \ddots & \vdots \\ & & & & \ddots & h_H \\ & & & & & 0 \\ & & & & & \vdots \\ 0 & \cdots & & & & 0 \end{bmatrix}, \quad (24)$$

while in case of overlapped prefix and suffix, as in Figure 2b, $\mathbf{H}_2$ is

$$\mathbf{H}_2 = \begin{bmatrix} 0 & \cdots & 0 & h_H & \cdots & h_{L_{\text{pre}}+2} \\ \vdots & & & & \ddots & \vdots \\ & & & & \ddots & h_H \\ & & & & & 0 \\ & & & & & \vdots \\ 0 & \cdots & & & & 0 \end{bmatrix}. \quad (25)$$

The received data (22) then becomes

$$\begin{aligned} \mathbf{r}_i &= \mathbf{F}\mathbf{H}_1(\mathbf{T}_1\tilde{\mathbf{u}}_i + \mathbf{T}_2\hat{\mathbf{u}}_i + \mathbf{T}_3\check{\mathbf{u}}_i) \\ &\quad + \mathbf{F}\mathbf{H}_2(\mathbf{T}_1\tilde{\mathbf{u}}_{i-1} + \mathbf{T}_2\hat{\mathbf{u}}_{i-1} + \mathbf{T}_3\check{\mathbf{u}}_{i-1}) \\ &= \mathbf{F}\mathbf{H}_1\mathbf{T}_1\mathbf{F}^H\tilde{\mathbf{d}}_i + \mathbf{F}\mathbf{H}_1\mathbf{T}_2\mathbf{F}^H\hat{\mathbf{d}}_i + \mathbf{F}\mathbf{H}_1\mathbf{T}_3\mathbf{F}^H\check{\mathbf{d}}_i \\ &\quad + \mathbf{F}\mathbf{H}_2\mathbf{T}_1\mathbf{F}^H\tilde{\mathbf{d}}_{i-1} + \mathbf{F}\mathbf{H}_2\mathbf{T}_2\mathbf{F}^H\hat{\mathbf{d}}_{i-1} \\ &\quad + \mathbf{F}\mathbf{H}_2\mathbf{T}_3\mathbf{F}^H\check{\mathbf{d}}_{i-1}. \quad (26) \end{aligned}$$

By substituting $\tilde{\mathbf{d}}_i$, $\hat{\mathbf{d}}_i$ and $\check{\mathbf{d}}_i$ using (4) and extracting the desired part of the signal we obtain

$$\mathbf{r}_i = \mathbf{F}\mathbf{H}\mathbf{F}^H\mathbf{d}_i + (\mathbf{F}\mathbf{H}_1\mathbf{T}_1\mathbf{F}^H\tilde{\mathbf{G}} + \mathbf{F}\mathbf{H}_1\mathbf{T}_2\mathbf{F}^H\hat{\mathbf{G}} - \mathbf{F}\mathbf{H}\mathbf{F}^H)\mathbf{d}_i + (\mathbf{F}\mathbf{H}_2\mathbf{T}_1\mathbf{F}^H\tilde{\mathbf{G}} + \mathbf{F}\mathbf{H}_2\mathbf{T}_3\mathbf{F}^H\check{\mathbf{G}})\mathbf{d}_{i-1},$$

where $\mathbf{H}$ is the circular channel convolution matrix. Here, the first term is the desired signal, the second term includes the channel-induced ICI and the transmitter-induced ISI by precoder $\tilde{\mathbf{G}}$. By extracting the transmitter-induced ICI, which we will refer to as self-ICI, $\mathbf{r}_i$ becomes

$$\begin{aligned}\mathbf{r}_i &= \mathbf{F}\mathbf{H}\mathbf{F}^H\mathbf{d}_i + \mathbf{F}\mathbf{H}\mathbf{F}^H(\tilde{\mathbf{G}} - \mathbf{I})\mathbf{d}_i \\ &\quad + (\mathbf{F}(\mathbf{H}_1\mathbf{T}_1 - \mathbf{H})\mathbf{F}^H\tilde{\mathbf{G}} + \mathbf{F}\mathbf{H}_1\mathbf{T}_2\mathbf{F}^H\hat{\mathbf{G}})\mathbf{d}_i \\ &\quad + (\mathbf{F}\mathbf{H}_2\mathbf{T}_1\mathbf{F}^H\tilde{\mathbf{G}} + \mathbf{F}\mathbf{H}_2\mathbf{T}_3\mathbf{F}^H\check{\mathbf{G}})\mathbf{d}_{i-1}. \qquad (27)\end{aligned}$$

Therefore, finally, the received signal in (27) becomes

$$\mathbf{r}_i = \mathbf{D}\mathbf{d}_i + \mathbf{G}_{\text{self-ICI}}\mathbf{d}_i + \mathbf{G}_{\text{ICI}}\mathbf{d}_i + \mathbf{G}_{\text{ISI}}\mathbf{d}_{i-1}, \qquad (28)$$

where

$$\begin{aligned}\mathbf{D} &= \text{diag}(\mathbf{F}\mathbf{h}) = \mathbf{F}\mathbf{H}\mathbf{F}^H, \\ \mathbf{G}_{\text{self-ICI}} &= -\mathbf{D}(\mathbf{I} - \tilde{\mathbf{G}}), \\ \mathbf{G}_{\text{ICI}} &= -(\mathbf{F}\Lambda_0\mathbf{F}^H\tilde{\mathbf{G}} - \mathbf{F}\Lambda_{12}\mathbf{F}^H\hat{\mathbf{G}}), \\ \mathbf{G}_{\text{ISI}} &= \mathbf{F}\Lambda_{21}\mathbf{F}^H\tilde{\mathbf{G}} + \mathbf{F}\Lambda_{23}\mathbf{F}^H\check{\mathbf{G}}. \qquad (29)\end{aligned}$$

Here $\Lambda_{ij} = \mathbf{H}_i\mathbf{T}_j$, for $i, j = 1, 2, 3$ and $\Lambda_0 = \mathbf{H} - \Lambda_{11}$.

The first term in (28) is the desired signal, the second term is the additive interference caused by the precoder and the third and fourth terms represent the ICI and ISI due to the channel, respectively.

We assume that the data is uncorrelated, $E\{\mathbf{d}_i\mathbf{d}_i^H\}=\mathbf{I}_K$ and $E\{\mathbf{d}_i\mathbf{d}_j^H\}=\mathbf{0}_K$ if $i\neq j$. The covariance matrix of the self-ICI-term in (28), $\mathbf{G}_{\text{self-ICI}}\mathbf{d}_i$, becomes

$$\begin{aligned}\mathbf{C}_{\text{self-ICI}} &\overset{\text{def}}{=} E\{\mathbf{G}_{\text{self-ICI}}\mathbf{d}_i\mathbf{d}_i^H{\mathbf{G}_{\text{self-ICI}}}^H\} \\ &= E\{\mathbf{G}_{\text{self-ICI}}{\mathbf{G}_{\text{self-ICI}}}^H\}. \qquad (30)\end{aligned}$$

Similarly, the covariance matrix of the channel-induced ISI and ICI-term in (28), are

$$\mathbf{C}_{\text{ISI}} = E\{\mathbf{G}_{\text{ISI}}{\mathbf{G}_{\text{ISI}}}^H\} \quad \text{and} \quad \mathbf{C}_{\text{ICI}} = E\{\mathbf{G}_{\text{ICI}}{\mathbf{G}_{\text{ICI}}}^H\}, \qquad (31)$$

respectively. The diagonal elements of these covariance matrices contain the interference power of the respective subcarrier, $\mathbf{P}_{\text{self-ICI},k}=[\mathbf{C}_{\text{self-ICI}}]_{kk}$,$\mathbf{P}_{\text{ICI},k}=[\mathbf{C}_{\text{ICI}}]_{kk}$ and $\mathbf{P}_{\text{ISI},k}=[\mathbf{C}_{\text{ISI}}]_{kk}$.

The total self-ICI power is the trace of $\mathbf{C}_{\text{self-ICI}}$, $\mathbf{P}_{\text{self-ICI,total}} = \text{Tr}\{\mathbf{C}_{\text{self-ICI}}\}$, and similarly, the total ISI and ICI power are $\mathbf{P}_{\text{ISI,total}} = \text{Tr}\{\mathbf{C}_{\text{ISI}}\}$ and $\mathbf{P}_{\text{ICI,total}} = \text{Tr}\{\mathbf{C}_{\text{ICI}}\}$, respectively.

Furthermore, ISI is always uncorrelated with ICI and self-ICI as $E\{\mathbf{d}_i\mathbf{d}_{i-1}^H\}=\mathbf{0}_K$, albeit in general ICI and self-ICI are correlated. We can show that in case of symbol precoding in [13] ($\tilde{\mathbf{G}} = \check{\mathbf{G}}$) ICI and self-ICI are also uncorrelated.

Note that, importantly, in case of prefix and prefix/suffix precoding ($\tilde{\mathbf{G}} = \mathbf{I}$) self-ICI becomes zero, see (29) and (30). Therefore, the total interference power in these systems becomes

$$\mathbf{P}_{\text{total}} = \mathbf{P}_{\text{ISI,total}} + \mathbf{P}_{\text{ICI,total}} + \mathbf{P}_{\text{self-ICI,total}}. \qquad (32)$$

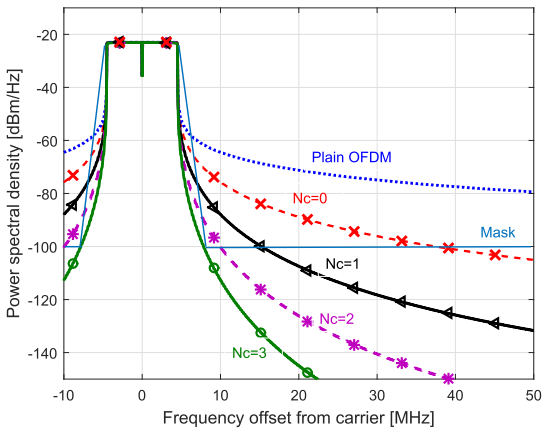

Fig. 3. The power spectrum of the plain OFDM, symbol precoding in [13], prefix precoding in [14] and prefix/suffix precoding for $N_c = 0$ to 3 and T_{pre}=T_{suf}=2.35μs. For all evaluated N_c the results of conventional symbol precoding in [13], prefix precoding in [14] and prefix/suffix precoding are indistinguishable.

Equation (32) shows that in a case of non-dispersive channel, the interference is zero because the precoder does not change the data symbol in the useful part. This is a valuable and key improvement over [13] where self-interference induced by the precoder regardless of the channel exists. The amount of interference in case of dispersive channels depends on the channel and also the precoder, $\tilde{\mathbf{G}}$. In the next section we evaluate the interference in the proposed system and design the system in order to have good OOB emission with minimum amount of interference.

VI. Simulation Results

In this section we investigate the design of the prefix/suffix precoding system. We evaluate the OOB emission and the interference that occur in our system and compare them with symbol precoding in [13] and prefix precoding in [14]. We consider LTE parameters for 10MHz channel bandwidth with 600 subcarriers, a sampling frequency of 15.36 MHz, 1024 samples of the symbol with the length of $T_s = 66.7\mu$s and 72 samples of the cyclic prefix with the length of $T_g = 4.7\mu$s [23]. Prefix/suffix precoding uses the scheme in Figure 2a where T_{suf}=βT_g and T_{pre}=$(1-\beta)T_g$, $0<\beta<1$. Prefix precoding uses the scheme in Figure 2b with T_{pre}=T_{suf}=T_g and in symbol precoding T_{suf}=0 and T_{pre}=T_g.

Figure 3 shows the power spectrum (19) of the plain OFDM, symbol precoding in [13], prefix precoding in [14] and prefix/suffix precoding for $N_c = 0$, 1, 2, 3. Although for all evaluated values of N_c the results of symbol precoding in [13], prefix precoding in [14] and proposed method are indistinguishable, we have not been able to formally prove their equality. Moreover, the spectrum does hardly change for different lengths T_{pre} and T_{suf}. Based on results not shown in the Figure, only in case of extremely short T_{pre} and T_{suf} where not enough space remains to construct continuity between symbols, OOB emission is higher.

Figure 4 shows the average normalized interference power, (32), in several multipath fading channels represented in Figure 5 for suffix length of 0 to full size, 4.7μs. Since,

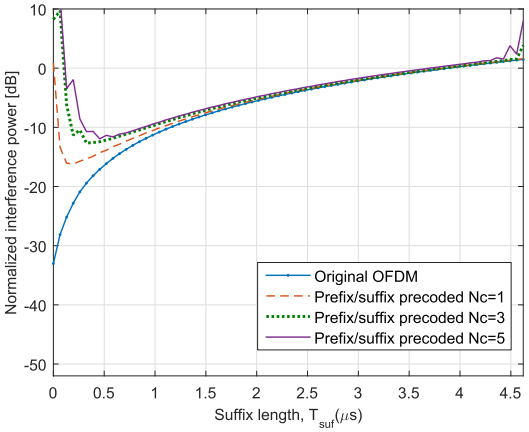

(a) α=0

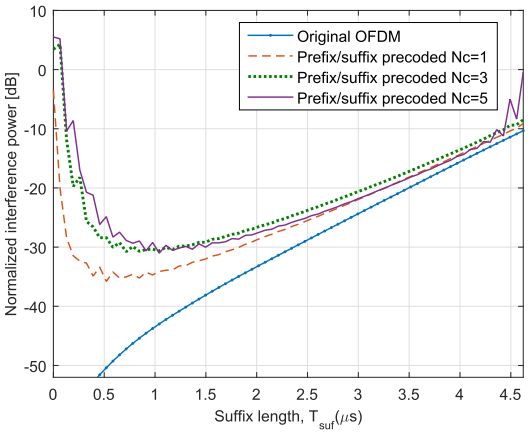

(b) α=1

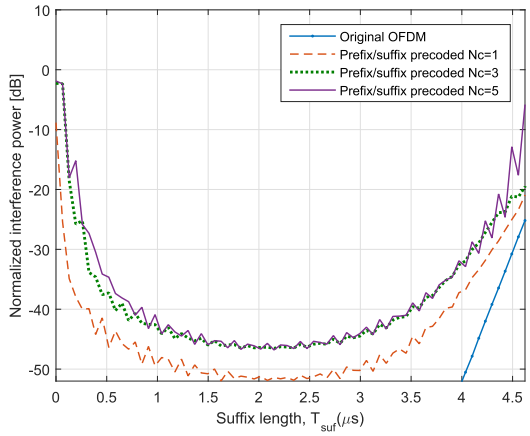

(c) α=5

Fig. 4. Average normalized interference power in multipath channel with an exponentially decaying power delay profile of $e^{-\alpha t}$, $0 < t < 4.7\mu$s, as in Figure 5. T_{pre}=$T_g - T_{\text{suf}}$ and T_g=$4.7\mu s$

the spectrum does not depend on the the size of prefix or suffix, we share the guard interval between the prefix and suffix in a way to cause as minimum interference as possible. In other words, we are looking for a particular fraction β, T_{suf}=βT_g and T_{pre}=$(1-\beta)T_g$, that minimizes $\mathbf{P}_{\text{total}}$ in (32) for a given channel decay characteristic α. Figure 4 shows that in case of channels with more dispersion (smaller α), minimum interference occurs for a shorter suffix. This short length of the suffix depends on the continuity order N_c and

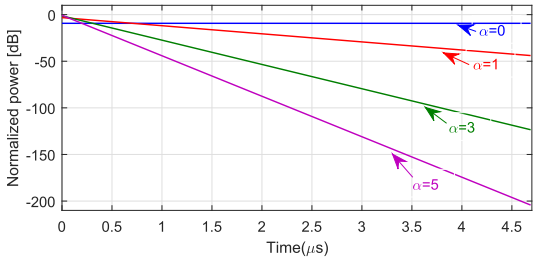

Fig. 5. Power delay profile of $h(t) = e^{-\alpha t}$, $0 < t < 4.7\mu$s and zero otherwise for $\alpha = 0$, 1, 3 and 5.

on the channel decay characteristic α. Moreover, for a very short suffix not only the interference level increases but also the OOB emission increases. Therefore, we conclude that the most proper suffix length to provide N-continuity is one that leads to the minimum interference level.

When the channel approaches a one-tap channel (large α), for instance $\alpha = 5$ in Figure 5, there is no need for a prefix to prevent ISI and ICI. In such case, the only purpose of having prefix and suffix is to force the signal's continuity. Therefore, the optimal lengths of suffix and prefix are equal and occur in the middle of the guard interval, see Figure 4c.

On the other hand, in practice, in a case that the interference is approximately less than -20dB, the electronic/RF noise is dominating the interference. In such a case, there is no practical need to decrease the interference. All the curves in Figure 4 suggest that having a suffix with the length of at most 0.5μs is enough to have a good performance even in case of more dispersive channels (smaller α). This is the optimal choice in case of not having any knowledge about how dispersive the channel is.

Figure 6 shows the interference power (32) that occurs in symbol precoding in [13], prefix precoding in [14] and prefix/suffix precoding system with T_{suf}=$0.3\mu s$ for different dispersive channels (different αs) and for $N_c = 1$, 3 and 5. For all channels, prefix precoding and the proposed method cause less interference than symbol precoding as in these systems the useful part of the symbol remains unchanged and therefore the self-interference, which exists in symbol precoding, is eliminated in prefix precoding and in the proposed prefix/suffix precoding method. Furthermore, for small α or a more dispersive channel, the proposed method causes less interference than prefix precoding. Even though in case of large α, the interference power for prefix precoding is less than for our method, the range of the interference power suggests no practical difference between prefix precoding and the proposed method.

Figure 7 shows MSE in symbol's extension part by the proposed method,

$$e(t) = \begin{cases} \dfrac{\left|s_{i-1}^{\text{plain}}(t) - s_{i-1}^{\text{precoded}}(t)\right|^2}{\|s_{i-1}^{\text{plain}}(t)\|_2^2} & -T_{\text{g}} \le t < -T_{\text{pre}} \\ \dfrac{\left|s_{i}^{\text{plain}}(t) - s_{i}^{\text{precoded}}(t)\right|^2}{\|s_{i}^{\text{plain}}(t)\|_2^2} & -T_{\text{pre}} \le t < 0, \end{cases} \tag{33}$$

for $T_{\text{pre}} = 3.25\mu$s, $T_{\text{suf}} = 1.45\mu$s, where $s_i^{\text{plain}}(t)$ represents the ith transmitted signal, $s_i(t)$ in (2), with $\tilde{\mathbf{G}} = \bar{\mathbf{G}} = \mathbf{I}$

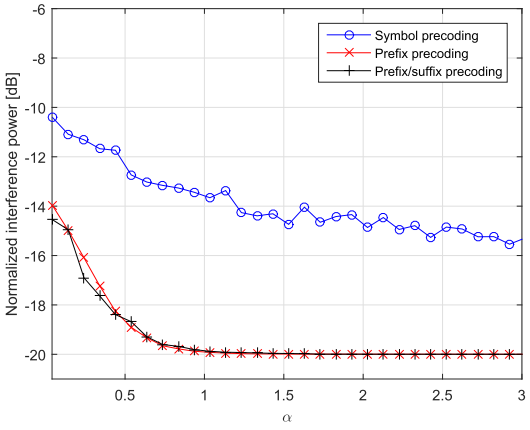

(a) N_c=1

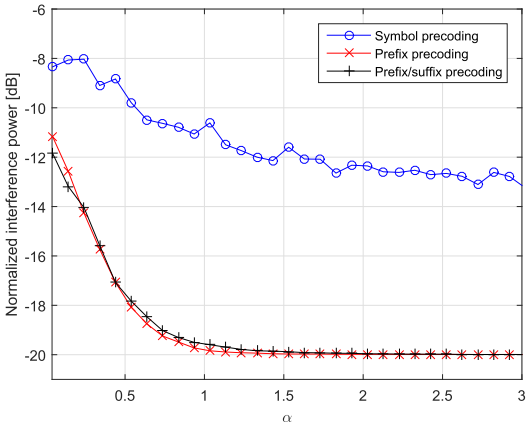

(b) N_c=3

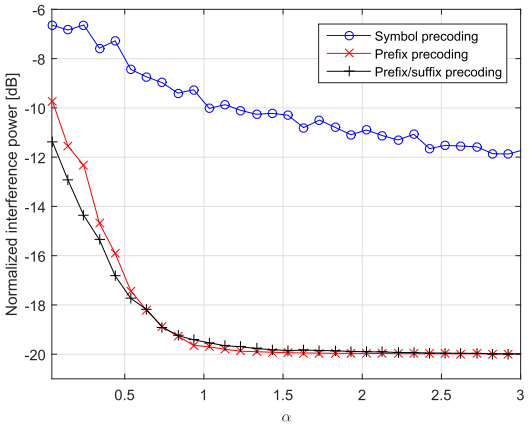

(c) N_c=5

Fig. 6. Average normalized interference power for a) $N_c = 1$, b) $N_c = 3$, c) $N_c = 5$ where T_{suf}=0.3μs.

and $s_i^{\text{precoded}}(t)$ is the ith transmitted signal in the suffix/prefix precoded system with $N_c = 3$. The result is averaged over a large number of symbols (10000 symbols). The error power, $e(t)$, in the useful part of the symbol (from 0 to 66.7μs) is zero and any changes compared to the plain OFDM symbol are constrained in the extension part, mostly in the region where the suffix and prefix join, $t = -3.25\mu$s in Figure 7. It is what we expected as our goal in designing the precoder in Section III-B was to change the symbol just in the extension part. We see that the averaged relative error power is extremely low and therefore, the prefix and suffix are *almost* cyclic. This motivates the use of the notion of *quasi-cyclic* prefix and suffix.

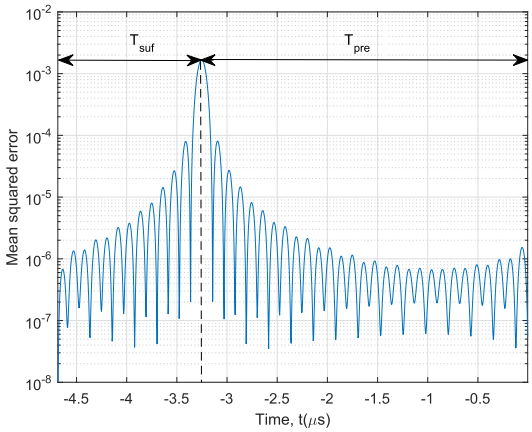

Fig. 7. MSE in a symbol by prefix/suffix precoder.

VII. Sum-Rate

In this section we evaluate the achievable rate of prefix/suffix precoding on a frequency selective channel. In our evaluations, channel is a frequency selective channel with power delay profile of $h(t) = e^{-\alpha t}$, $0 < t < 2.7\mu$s and zero otherwise, thermal noise is Gaussian distributed with zero mean and variance σ^2 and signal-to-noise ratio is SNR=$\frac{1}{\sigma^2}$. The result is averaged over 1000 channel realizations. We define

$$R \triangleq E\{\log_2[\det(\mathbf{I} + \text{SINR})]\}, \tag{34}$$

where R is an achievable rate of the system, expectation, $E\{\cdot\}$, is over all channel realizations and SINR is the signal-to-interference-plus-noise ratio,

$$\text{SINR}= \left[\mathbf{D}\mathbf{D}^H\right] (\sigma^2\mathbf{I} + [\mathbf{C}_{\text{self-ICI}}] + [\mathbf{C}_{\text{ICI}}] + [\mathbf{C}_{\text{ISI}}])^{-1}. \tag{35}$$

where matrices $\mathbf{D}$, $\mathbf{C}_{\text{self-ICI}}$, $\mathbf{C}_{\text{ICI}}$ and $\mathbf{C}_{\text{ISI}}$ are calculated using (29)–(31).

Figure 8 shows the evaluated rate for plain OFDM, symbol precoding with $N_c = 4$, prefix/suffix precoding with $N_c = 4$ and $\beta = 1/3$ and root-raised cosine (RRC) windowing where the whole guard interval is used to apply the window [9]. The interference analysis of the windowed OFDM is explain in [9]. Note that, in windowing, as long as the useful part of the symbol is untouched there is no self-ICI.

In practical systems, receivers apply per-subcarrier processing. With this restriction sum-rate becomes

$$R \triangleq \sum_{k=1}^{K} E\{\log_2(1 + \text{SINR}_k)\}, \tag{36}$$

where expectation, $E\{\cdot\}$, is over all channel realizations and SINR_k is the signal-to-interference-plus-noise ratio on k^{th} subcarrier,

$$\text{SINR}_k = \frac{\left[\mathbf{D}\mathbf{D}^H\right]_{kk}}{\sigma^2 + [\mathbf{C}_{\text{self-ICI}}]_{kk} + [\mathbf{C}_{\text{ICI}}]_{kk} + [\mathbf{C}_{\text{ISI}}]_{kk}}. \tag{37}$$

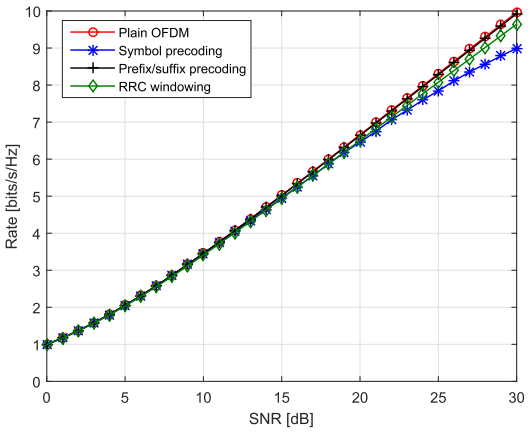

Fig. 8. Sum-rate of plain OFDM, symbol precoding with $N_c = 4$, prefix/suffix precoding with $N_c = 4$ and $\beta = 1/3$ and RRC windowing, considering correlated subcarriers.

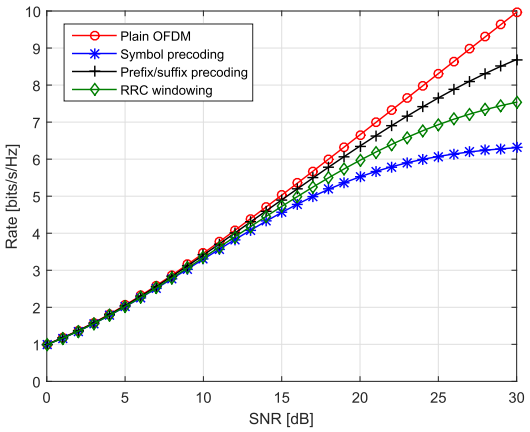

Fig. 9. Sum-rate of plain OFDM, symbol precoding with $N_c = 4$, prefix/suffix precoding with $N_c = 4$ and $\beta = 1/3$ and RRC windowing, ignoring the correlation between subcarriers.

In (37) we just account for the diagonal elements of the matrices which contain the information on each subcarriers reflecting a transmitter/receiver unaware of any interchannel correlations.

Figure 9 shows the rate evaluation of (36). We see that in symbol precoding the sum-rate is degraded, specially at high SNR scenarios while in the suffix/prefix precoded system the rate-loss is very small. This is because of no self-interference in prefix/suffix precoding technique. Moreover, RRC windowing also degrades the capacity because the data in windowed part changes relatively a lot. Prefix/suffix precoder finds the optimal modification to the prefix and suffix parts and does not change the useful part of the symbol. This is the key factor to maintain the rate.

VIII. Discussion

A. N-Continuous OFDM Versus Transmit-Windowed OFDM

Windowing is a classical means to suppress the OOB emission by simply applying a smooth window to the OFDM symbol in order to make the smooth transition between OFDM symbols which causes fast decaying sinc-shaped subcarriers.

Windowing in order to suppress the OOB emission comes with a price. The price is either losing the spectral efficiency by extending the required transition gap between the consecutive symbols, see Figure 10a, or additional ISI due to overlapping the current symbol in prefix part with the previous symbol's suffix part and the ICI due to changing the data in prefix part of the symbol, see Figure 10b, [9]. The concept of overlapping a shaped prefix and suffix is introduced in 90s for VDSL [24] and recently, suggested for the 5G [25]. Here, we assume that the transition occurs in prefix and suffix part of the symbol as illustrated in Figure 10b.

Some studies have been done on the window shape to reduce the price that may occur. For instance, in [9] and [10] asymmetric window shape is suggested to reduce the introduced ISI and ICI by the window. A thorough analysis on ISI and ICI in a windowed OFDM system is presented in [9]. In [26] an enhanced variant of windowing is proposed where different windows with different lengths are applied to different groups of subcarriers.

N-continous OFDM and windowing have some similarities. In windowing method, OFDM symbols typically become N-continous. The window modifies the data symbol to construct the smooth transition at its discontinuous edges. Smoothing the data symbol makes it continuous. the order of continuity depends on the particular window shape. For instance, for the well-known raised cosine window (RC) the signal's continuity order is $N_c = 1$ since, at all edges:

$$\begin{aligned}
\frac{d^n}{dt^n} s_i^{\text{RC}}(t)\Big|_{t=-T_{\text{pre}}} &= 0,\\
\frac{d^n}{dt^n} s_i^{\text{RC}}(t)\Big|_{t=T_s+T_{\text{suf}}} &= 0,\\
\frac{d^n}{dt^n} s_i^{\text{RC}}(t)\Big|_{t=T_s} &= \frac{d^n}{dt^n} s_i^{\text{plain}}(t)\Big|_{t=T_s}\\
\frac{d^n}{dt^n} s_i^{\text{RC}}(t)\Big|_{t=0} &= \frac{d^n}{dt^n} s_i^{\text{plain}}(t)\Big|_{t=0},
\end{aligned} \tag{38}$$

for $n \in \{0, 1\}$, where $s_i^{\text{RC}}(t) = s_i^{\text{plain}}(t) w_{\text{RC}}(t)$ and $w_{\text{RC}}(t)$ is the raised cosine window shape [9],

$$w_{\text{RC}}(t) = \begin{cases} \cos^2\left(\dfrac{\pi(t+T_{\text{pre}}-T_w)}{2T_w}\right), & -T_{\text{pre}} \leqslant t < -T_{\text{pre}}+T_w \\ 1, & -T_{\text{pre}}+T_w \leqslant t < T_s+T_{\text{suf}}-T_w \\ \cos^2\left(\dfrac{\pi(t-T_s-T_{\text{suf}}+T_w)}{2T_w}\right), & T_s+T_{\text{suf}}-T_w \leqslant t < T_s+T_{\text{suf}} \\ 0, & Otherwise. \end{cases} \tag{39}$$

For the root-raised cosine window (RRC) the signal's continuity order is $N_c = 0$ since,

$$\begin{aligned}
\frac{d^n}{dt^n} s_i^{\text{RRC}}(t)\Big|_{t=-T_{\text{pre}}} &= 0,\\
\frac{d^n}{dt^n} s_i^{\text{RRC}}(t)\Big|_{t=T_s+T_{\text{suf}}} &= 0,\\
\frac{d^n}{dt^n} s_i^{\text{RRC}}(t)\Big|_{t=T_s} &= \frac{d^n}{dt^n} s_i^{\text{plain}}(t)\Big|_{t=T_s}\\
\frac{d^n}{dt^n} s_i^{\text{RRC}}(t)\Big|_{t=0} &= \frac{d^n}{dt^n} s_i^{\text{plain}}(t)\Big|_{t=0},
\end{aligned} \tag{40}$$

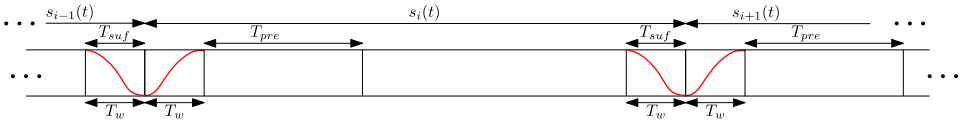

(a) Head part of the window is applied on an extra extenssion part and prefix remains unchanged. The tail part of the window is applied on the suffix part. OFDM symbols do not overlap.

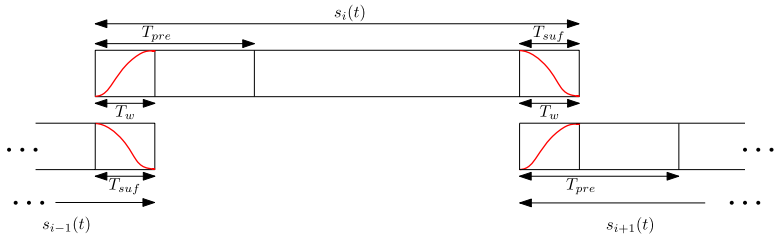

(b) Part of prefix is used to apply the head part of the window. The tail part of the window is applied on the suffix part. Two consecutive OFDM symbols overlap over the window parts [24].

Fig. 10. Consecutive windowed OFDM symbols in the time domain. The head and the tail part of OFDM symbol are shaped by a window. T_w is the window length.

for $n = 0$. where, $s_i^{\text{RRC}}(t) = s_i^{\text{plain}}(t) w_{\text{RRC}}(t)$ and $w_{\text{RRC}}(t)$ is the root-raised cosine window shape [9], $w_{\text{RRC}}(t) = \sqrt{w_{\text{RC}}(t)}$.

While the precoder finds the optimal modification a window usually changes the data in windowed part relatively a lot. For instance, precoders in (5), (7) and (16) are found subject to minimum manipulation to the data in Euclidean sense. The precoder is particularly designed to make the minimum changes to the data while providing the required smoothness or continuity. Therefore, the increased channel-induced interference in precoding system is less than the increased channel-induced interference caused by windowing [9].

Moreover, windowing uses the whole prefix and suffix to construct the continuity while in precoding most of the changes occur at the boundaries of consecutive symbols, see Figure 7, and the data which are more close to the edges tolerate more error or modification which are basically just a few sample close to each edge. So shortening the prefix and suffix in a precoding system does not restrict making the signal continuous as far as a few samples exist to construct the continuity. While in windowing the whole prefix and suffix parts are used to make the smooth transition, shortening the prefix and suffix sharpen the transition and increases the OOB emission [9]. Figure 11 shows the power spectrum of plain OFDM, N-continuous precoded OFDM with $N_c = 4$ and RRC windowed OFDM where the whole guard interval is used for windowing, $T_w = T_g$. By shortening the guard interval OOB emission increases in the windowed OFDM, while, shortening the guard interval does not affect the OOB emission suppression in the N-continuous precoded system, as long as a few samples exist to construct the continuity. Note that the power spectrum of the symbol, prefix and prefix/suffix precoders, for the same order of continuity, N_c, are indistinguishable, see Figure 3. So, in comparison with precoding, in windowing technique more samples are required to make the signal continuous. Therefore, in windowing the OOB emission strongly depends on the prefix and suffix lengths [9] while in N-continuous OFDM, OOB emission does not depend on the prefix and suffix lengths. As a result,

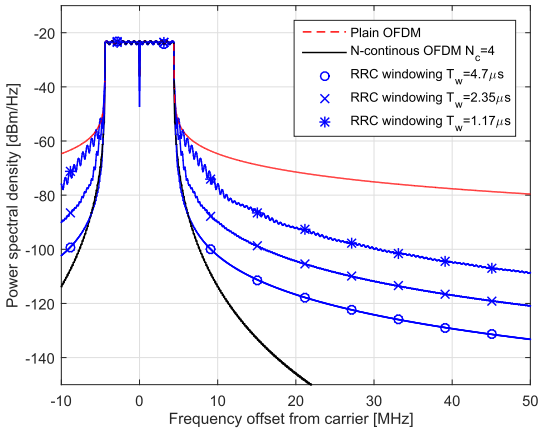

Fig. 11. The power spectrum of the RRC windowed OFDM with $T_w = T_g$, prefix/suffix precoding with $N_c = 4$ and $\beta = 1/3$ for $T_g = 4.7$, 2.35 and 1.17μs. For all evaluated T_g the results of prefix/suffix are indistinguishable.

unlike in windowing, in precoding shortening the prefix and suffix overhead is relatively easy. This is a key improvement for low-latency systems.

B. PAPR

Besides high OOB, high Peak-to-Average Power Ratio (PAPR) is another main shortcomings of OFDM signals for cognitive radios. High peaks of OFDM occur when sinusoidal signals of the OFDM subcarriers are added constructively. The constructive addition of the subcarriers which happen irregularly result in high PAPR. These high peaks limits the operation of linear power amplifiers due to amplifier saturation leading to non-linearity and distortion. Therefore, larger and expensive power amplifiers are needed to deal with the high PAPR.

We define the PAPR of the transmitted signal in (1) as

$$\text{PAPR} = \frac{\max |s(t)|^2}{\frac{1}{T}\int_{t=-T_g}^{T_s} |s(t)|^2}. \tag{41}$$

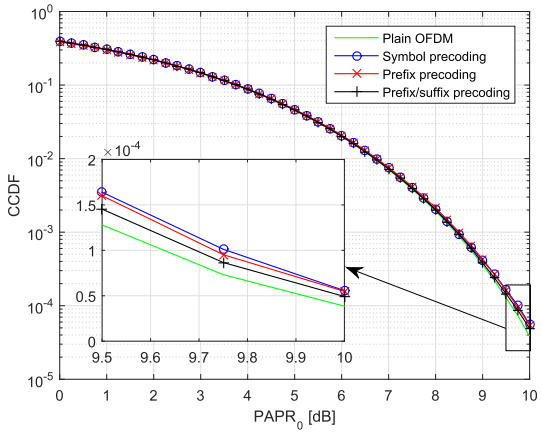

Fig. 12. CCDFs of PAPR of plain OFDM and various precoding techniques with $N_c = 4$.

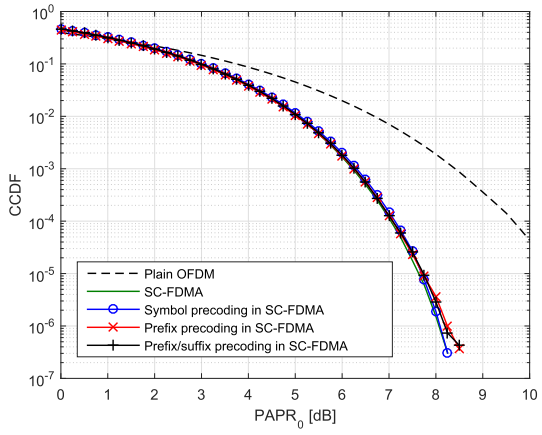

Fig. 13. CCDFs of PAPR of plain OFDM and various precoding techniques with $N_c = 4$ in SC-FDMA.

Usually, complementary cumulative density function (CCDF) is considered to evaluate the PAPR of the system defined as

$$\text{CCDF} = \Pr(\text{PAPR} > \text{PAPR}_0), \tag{42}$$

which is the probability that PAPR is larger than some threshold level (PAPR_0).

Figure 12 shows the CCDF plots of plain, symbol precoded, prefix precoded and prefix/suffix precoded OFDM signals over 1000 random OFDM symbols. The figure shows that the PAPR characteristics of precoded systems are very similar to the PAPR characteristic of the plain OFDM. The curves do not change with changing the order of continuity, N_c.

In the literature there are various precoding methods to deal with PAPR issue. A joint precoder can be designed to suppress the OOB emission as well as reduce the PAPR, for instance in [27] an optimized PAPR precoder is designed for the symbol precoded system in [28]. The result, which is a cascade of the spectral precoder and the PAPR precoder, is a joint precoder that can be computed off-line. Another well-known solution to PAPR problem is single carrier frequency division multiple access (SC-FDMA) [29] where PAPR is reduced by introducing an FFT block just before the IFFT block in an OFDM system. This FFT block is an example of PAPR precoder. Figure 13 shows the PAPR in SC-FDMA along with symbol, prefix and prefix/suffix precoding. We see that even in SC-FDMA using spectral precoders does not affect PAPR.

TABLE I

ADDITIONAL COMPLEXITY OF VARIOUS PRECODING TECHNIQUES IN COMPARED TO PALIN OFDM

Method	Additional complexity to plain OFDM
Symbol precoding in [13]	$4(N_c+1)K$
Prefix precoding in [14]	$8(N_c+1)K$
Prefix/suffix precoding	$6(N_c+1)K$

C. Complexity

The complexity of the prefix precoder in [13] is mistakenly reported in the literature as K^2, while the complexity can be reduced to $4(N_c+1)K$ by decomposition of precoder matrix fully explained in [30].

Using the matrix decomposition leads to huge complexity reduction where K is large. The comparison of additional complexity of symbol precoding [13], prefix precoding [14] and prefix/suffix precoding to plain OFDM system is presented in Table I. We have shown that both prefix precoding and prefix/suffix precoding methods can be implemented in the order of K instead of K^2.

IX. CONCLUSION

In this paper we propose a new prefix/suffix OFDM precoder. The new precoder makes the system N-continuous without changing the useful part of the symbol which leads to low OOB emission while additive interference is less than other symbol precoding and prefix precoding OFDM systems. We also give a general analysis framework of the signal at the transmitter and receiver side which is applicable to many OFDM systems which are linearly precoded.

APPENDIX

Proof of Lemma 1: The transmitted prefix precoded signal in [14] is

$$s(t) = \sum_i s_i^p(t - i(T_s + T_g)) = \ldots + s_{i-1}^p(\tau + T_s + T_{\text{g}}) + s_i^p(\tau) + s_{i+1}^p(\tau - T_s - T_{\text{g}}) + \ldots \tag{43}$$

where $\tau = t - i(T_s + T_{\text{g}})$, $T_g = T_{\text{pre}}$ and $s_i^p(t)$ is the ith prefix precoded OFDM symbol,

$$s_i^p(t) = \sum_{k\in\kappa} d_{i,k} e^{j2\pi \frac{k}{T_s} t} I_{[0,T_s)}(t) + \sum_{k\in\kappa} d_{i,k}^{\text{pre}} e^{j2\pi} I_{[-T_g,0)}(t). \tag{44}$$

For brevity, we use the short notation of $F^{-1}\{\mathbf{d}_i\} \overset{\text{def}}{=} \sum_{k\in\kappa} d_{i,k} e^{j2\pi \frac{k}{T_s} t}$. Therefore,

$$\begin{aligned} s_i^p(t) &= F^{-1}\{\mathbf{d}_i\} I_{[0,T_s)}(t) + F^{-1}\{\mathbf{d}_i^{\text{pre}}\} I_{[-T_g,0)}(t) \\ &= F^{-1}\{\mathbf{d}_i\} I_{[0,T_s)}(t) + F^{-1}\{(\mathbf{I} - \mathbf{P})\mathbf{d}_i \\ &\quad + \mathbf{P}\mathbf{\Phi}^H \mathbf{d}_{i-1}\} I_{[-T_g,0)}(t). \end{aligned} \tag{45}$$

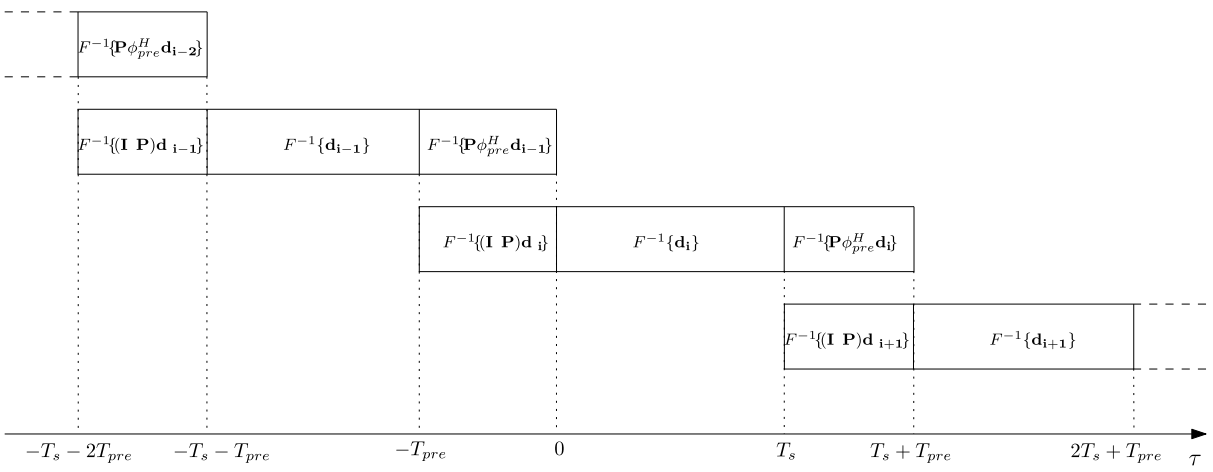

Fig. 14. Transmit prefix precoded OFDM signal in [14].

By substituting (7) in (45) and using the linear characteristic of the operation $F^{-1}\{.\}$, the transmitted signal becomes, see Figure 14,

$$\begin{aligned} s(t) &= \ldots + F^{-1}\{\mathbf{d}_{i-1}\}I_{[-T_s-T_g,-T_g)}(\tau) \\ &\quad + F^{-1}\{(\mathbf{I}-\mathbf{P})\mathbf{d}_{i-1}\}I_{[-T_s-2T_g,-T_s-T_g)}(\tau) \\ &\quad + F^{-1}\{\mathbf{P}\mathbf{\Phi}^{H}\mathbf{d}_{i-2}\}I_{[-T_s-2T_g,-T_s-T_g)}(\tau) \\ &\quad + F^{-1}\{\mathbf{d}_i\}I_{[0,T_s)}(\tau) + F^{-1}\{(\mathbf{I}-\mathbf{P})\mathbf{d}_i\}I_{[-T_g,0)}(\tau) \\ &\quad + F^{-1}\{\mathbf{P}\mathbf{\Phi}^{H}d_{i-1,k}\}I_{[-T_g,0)}(\tau) \\ &\quad + F^{-1}\{\mathbf{d}_{i+1}\}I_{[T_s+T_g,2T_s+T_g)}(\tau) + \ldots \\ &= \ldots + s_{i-1}(\tau) + s_i(\tau) + s_{i+1}(\tau) + \ldots \\ &= \sum_i s_i(t - i(T_s+T_g)), \end{aligned} \tag{46}$$

where,

$$\begin{aligned} s_i(t) = F^{-1}\{\mathbf{d}_i\}I_{[0,T_s)}(\tau) + F^{-1}\{(\mathbf{I}-\mathbf{P})\mathbf{d}_i\}I_{[-T_g,0)}(\tau) \\ + F^{-1}\{\mathbf{P}\mathbf{\Phi}^{H}\mathbf{d}_i\}I_{[T_s,T_s+T_g)}(\tau). \end{aligned}$$

This is identical to a ith transmitted prefix suffix precoded signal with the form of

$$\begin{aligned} s_i(t) = F^{-1}\{\tilde{\mathbf{G}}\mathbf{d}_i\}I_{[0,T_s)}(\tau) + F^{-1}\{\hat{\mathbf{G}}\mathbf{d}_i\}I_{[-T_{\text{pre}},0)}(\tau) \\ + F^{-1}\{\check{\mathbf{G}}\mathbf{d}_i\}I_{[T_s,T_s+T_{\text{suf}})}(\tau). \end{aligned} \tag{47}$$

■

REFERENCES

[1] B. Farhang-Boroujeny, "OFDM versus filter bank multicarrier," *IEEE Signal Process. Mag.*, vol. 28, no. 3, pp. 92–112, May 2011.

[2] V. Vakilian, T. Wild, F. Schaich, S. ten Brink, and J.-F. Frigon, "Universal-filtered multi-carrier technique for wireless systems beyond LTE," in *Proc. IEEE Globecom Workshops (GC Wkshps)*, Dec. 2013, pp. 223–228.

[3] N. Michailow *et al.*, "Generalized frequency division multiplexing for 5th generation cellular networks," *IEEE Trans. Commun.*, vol. 62, no. 9, pp. 3045–3061, Sep. 2014.

[4] Y. Cai, Z. Qin, F. Cui, G. Y. Li, and J. A. McCann, "Modulation and multiple access for 5G networks," *IEEE Commun. Surveys Tuts.*, vol. 20, no. 1, pp. 629–646, 4th Quart., 2018.

[5] *Final Report of 3GPP TSG RAN WG1 #86 v1.0.0 (Gothenburg, Sweden, 22-26 August 2016)*, document R1-1608562, MCCSupport, 3GPP TSG RAN WG1 Meeting #86bis, Lisbon, Portugal, Oct. 2016, pp. 68–69.

[6] M. Faulkner, "The effect of filtering on the performance of OFDM systems," *IEEE Trans. Veh. Technol.*, vol. 49, no. 5, pp. 1877–1884, Sep. 2000.

[7] T. Weiss, J. Hillenbrand, A. Krohn, and F. K. Jondral, "Mutual interference in OFDM-based spectrum pooling systems," in *Proc. IEEE 59th Veh. Technol. Conf. (VTC-Spring)*, vol. 4, May 2004, pp. 1873–1877.

[8] B. Farhang-Boroujeny and R. Kempter, "Multicarrier communication techniques for spectrum sensing and communication in cognitive radios," *IEEE Commun. Mag.*, vol. 46, no. 4, pp. 80–85, Apr. 2008.

[9] T. Taheri, R. Nilsson, and J. van de Beek, "Asymmetric transmit-windowing for low-latency and robust OFDM," in *Proc. IEEE Globecom Workshops (GC Wkshps)*, Dec. 2016, pp. 1–6.

[10] E. Güvenkaya, E. Bala, R. Yang, and H. Arslan, "Time-asymmetric and subcarrier-specific pulse shaping in OFDM-based waveforms," *IEEE Trans. Veh. Technol.*, vol. 64, no. 11, pp. 5070–5082, Nov. 2015.

[11] P. Sutton, B. Ozgul, I. Macaluso, and L. Doyle, "OFDM pulse-shaped waveforms for dynamic spectrum access networks," in *Proc. IEEE Symp. New Frontiers Dyn. Spectr. (DySPAN)*, Apr. 2010, pp. 1–2.

[12] J. van de Beek and F. Berggren, "N-continuous OFDM," *IEEE Commun. Lett.*, vol. 13, no. 1, pp. 1–3, Jan. 2009.

[13] J. van de Beek and F. Berggren, "EVM-constrained OFDM precoding for reduction of out-of-band emission," in *Proc. IEEE 70th Veh. Technol. Conf. Fall (VTC-Fall)*, Sep. 2009, pp. 1–5.

[14] H. Kawasaki, M. Ohta, and K. Yamashita, "N-continuous symbol padding OFDM for sidelobe suppression," in *Proc. IEEE Int. Conf. Commun. (ICC)*, Jun. 2014, pp. 5890–5895.

[15] Y. Zheng, J. Zhong, M. Zhao, and Y. Cai, "A precoding scheme for N-continuous OFDM," *IEEE Commun. Lett.*, vol. 16, no. 12, pp. 1937–1940, Dec. 2012.

[16] E. Gövenkaya, A. Şahin, and H. Arslan, "N-continuous OFDM with CP alignment," in *Proc. IEEE Mil. Commun. Conf. (MILCOM)*, Oct. 2015, pp. 587–592.

[17] H. Kawasaki, M. Ohta, and K. Yamashita, "Extension of N-continuous OFDM precoder matrix for improving error rate," *IEEE Commun. Lett.*, vol. 19, no. 2, pp. 283–286, Feb. 2015.

[18] A. Peled and A. Ruiz, "Frequency domain data transmission using reduced computational complexity algorithms," in *Proc. IEEE Int. Conf. Acoust., Speech, Signal Process. (ICASSP)*, vol. 5, Apr. 1980, pp. 964–967.

[19] *Series G: Transmission Systems and Media, Digital Systems and Networks, Fast Access to Subscriber Terminals (G.Fast) Physical Layer Specification*, document ITU-T G.9701, International Telecommunication Union Recommendation, Dec. 2014.

[20] *Evolved Universal Terrestrial Radio Access (E-UTRA); Physical Channels and Modulation (Release 13)*, document TSG RAN TS 36.211, 3GPP, v13.0.0., Dec. 2015. [Online]. Available: http://www.3gpp.org/

[21] F. Sjoberg, M. Isaksson, R. Nilsson, P. Odling, S. K. Wilson, and P. O. Borjesson, "Zipper: A duplex method for VDSL based on DMT," *IEEE Trans. Commun.*, vol. 47, no. 8, pp. 1245–1252, Aug. 1999.

[22] W. Chongburee, "Analysis of power spectral density of digitally-modulated combined pulse trains," in *Proc. 2nd Annu. Conf. Elect. Eng./Electron. Comput. Telecommun. Inf. Technol. (ECTI)*, 2005, pp. 469–472.

[23] *Evolved Universal Terr. Radio Access (E-UTRA); Base Station (BS) radio Transmiss. reception (Release 13)*, document TSG RAN TS 36.104, 3GPP, v13.0.0., Jan. 2016. [Online]. Available: http://www.3gpp.org/
[24] F. Sjoberg, R. Nilsson, M. Isaksson, P. Odling, and P. O. Borjesson, "Asynchronous zipper [subscriber line duplex method]," in *Proc. IEEE Int. Conf. Commun. (ICC)*, vol. 1, Jun. 1999, pp. 231–235.
[25] A. A. Zaidi *et al.*, "Waveform and numerology to support 5G services and requirements," *IEEE Commun. Mag.*, vol. 54, no. 11, pp. 90–98, Nov. 2016.
[26] A. Sahin and H. Arslan, "Edge windowing for OFDM based systems," *IEEE Commun. Lett.*, vol. 15, no. 11, pp. 1208–1211, Nov. 2011.
[27] J. Fang and I.-T. Lu, "Precoder designs for jointly suppressing out-of-band emission and peak-to-average power ratio in an orthogonal frequency division multiplexing system," *IET Commun.*, vol. 8, no. 10, pp. 1705–1713, Jul. 2014.
[28] J. van de Beek, "Orthogonal multiplexing in a subspace of frequency well-localized signals," *IEEE Commun. Lett.*, vol. 14, no. 10, pp. 882–884, Oct. 2010.
[29] H. G. Myung, J. Lim, and D. J. Goodman, "Single carrier FDMA for uplink wireless transmission," *IEEE Veh. Technol. Mag.*, vol. 1, no. 3, pp. 30–38, Sep. 2006.
[30] M. Mohamad, R. Nilsson, and J. van de Beek, "Minimum-EVM N-continuous OFDM," in *Proc. IEEE Int. Conf. Commun. (ICC)*, May 2016, pp. 1–5.

Tayebeh Taheri received the B.S. degree in electronics engineering from Shahid Beheshti University, Tehran, Iran, in 2008, and the M.S. degree in electronics engineering from Tarbiat Modares University, Tehran, in 2012. She is currently pursuing the Ph.D. degree with the Signal Processing Group, Department of Computer Science, Electrical and Space Engineering, LuleåUniversity of Technology, Sweden. Her research focus is on physical layer for radio communications, multi-carrier wireless technologies, waveform designs, and interference cancellation in MIMO systems.

Rickard Nilsson received the M.Sc., Lic.Eng., and Ph.D. degrees in CS&EE and signal processing from the LuleåUniversity of Technology (LTU), Sweden. With Telia Research AB, Sweden, and Stanford University, Stanford, CA, USA, he developed and researched a new broadband access technology for VDSL and contributed to its standardization; a successful technology which enabled true broadband Internet access to many millions of homes and offices worldwide over existing telephone wires. For seven years, he researched broadband access technologies at the Telecommunications Research Center Vienna (ftw.), Austria, in close cooperation with telecom operators, system- and semiconductor manufacturers. He was also a Lecturer with Technical University, Vienna, and co-supervised Ph.D. students. In 2010, he returned to LTU and founded a new research group with wireless communications and software-defined radio and established new research cooperation with mining, telecom, and space industries. At LTU, he continues to lecture signal processing and communications courses, perform research, and supervise Ph.D. students.

Jaap van de Beek (S'94–M'06–SM'14–F'17) is Chaired Professor of signal processing with Luleå University of Technology, Sweden. Prior to returning to academia in 2013, he spent over two decades in industry, in telecommunications research labs with Telia Research, Nokia Networks, and for more than twelve years with Huawei Technologies. In different roles, he has been involved in three generations of mobile cellular communications systems. He developed base station receiver algorithms for GSM evolution systems. He was among those pioneering OFDM as an access scheme for cellular radio in a standard proposal for the third-generation systems in 1997. From 2004 to 2009, he was contributing to the preparation and specification of 3GPP's fourth-generation LTE standard, for which he holds a number of essential patents. More recently, he has been developing methods that efficiently reduce spectral interference of radio transmitters, work for which he received the IEEE Communications Society Heinrich Hertz Award. Since 2012, he has been engaged in improving Internet access, wireless network connectivity, and cellular radio coverage in rural and remote regions.